Structure and magnetism of lanthanum clusters

Andrey Lyalin,* Andrey V. Solov'yov,† and Walter Greiner
Frankfurt Institute for Advanced Studies, Johann Wolfgang Goethe-University, Max von Laue Strasse 1, 60438 Frankfurt am Main, Germany
(Received 8 June 2006; published 11 October 2006)

The optimized structure, electronic and magnetic properties of La clusters consisting of up to 14 atoms have been investigated using *ab initio* theoretical methods based on density-functional theory. Structural and spin isomers have been determined. We show that increase in cluster symmetry can promote ferromagnetic instability in La clusters. A giant enhancement of magnetism in La_4, La_6, and La_{13} clusters is predicted. We also found that the ground states of La_2, La_3, La_5, La_7, La_9–La_{11}, and La_{14} clusters possess nonzero magnetic moments, that ranged from $\sim 0.1\mu_B$ to $1.0\mu_B$ per atom. Strong dependence of the magnetic moment on temperature for $T>300$ K is predicted. The results obtained are compared with the available experimental data and the results of other theoretical works.

DOI: 10.1103/PhysRevA.74.043201 PACS number(s): 36.40.Cg, 36.40.Mr, 31.10.+z, 31.15.Ne

I. INTRODUCTION

During the last two decades numerous theoretical and experimental efforts have been devoted to studying structural, electronic, optical and magnetic properties of atomic clusters (see, e.g., Refs. [1–5]). The properties of atomic clusters are very different from those of the bulk materials and change drastically with increasing cluster size. This fact gives a unique opportunity to form new materials by properly assembling selected clusters.

One of the most exciting developments in the physics of clusters relates to their magnetic behavior. Clusters exhibit novel magnetic properties essentially different from those of the corresponding bulk solids (see, e.g., Refs. [6,7] and references therein). The study of evolution of magnetic properties from atoms to the bulk is important for the development of magnetic nanomaterials and understanding the fundamental principles of spin coupling in finite and low dimensional systems.

The most explored type of magnetic clusters are the clusters of the ferromagnetic transition-metal elements, such as Fe, Co, Ni (see, e.g., Refs. [6–11] and references therein). Theoretically, a strong enhancement of magnetism in clusters of elements that are ferromagnetic as bulk solids was predicted [6,8,10]. The first experimental measurements of the magnetic moments of small free Fe, Co, and Ni clusters showed, however, that magnetization per atom was far less than the moment per atom in corresponding bulk material [12,13]. This contradiction was explained by relaxations of the magnetization of superparamagnetic clusters in the magnetic field [10,13]. Over the past years this model has been extensively used to interpret the experimental data [14].

Significant attention was paid to the Mn clusters, because Mn atom possess large magnetic moment due to the half-filled $3d$ electron shell. The magnetic moment of Mn atom is $5\mu_B$ (Bohr magneton), and, therefore, Mn clusters are good candidates for strong nanomagnets. The properties of Mn clusters are peculiar. The manganese dimer, Mn_2, is weakly bound, and while theoretical calculations predict ferromagnetic behavior [15,16], there is still question as to whether the coupling is actually ferromagnetic or it is antiferromagnetic, as it follows from the experimental data [16–18]. The small manganese clusters (Mn_3–Mn_8) are ferromagnetic [19–21] and possess large magnetic moments per atom [$(4–5)\mu_B$/atom], in spite of the fact that the most stable crystal structure of Mn exhibits antiferromagnetic behavior [22,23]. However, recent calculations combined with experimental study revealed that Mn_7 cluster posesses ferrimagnetic type of spin coupling [24]. The measured magnetic moment of Mn_7 is $(0.72\pm 0.42)\mu_B$/atom [24]. Larger manganese clusters (Mn_{11}–Mn_{99}) exhibit magnetic behavior that differs from either the smaller clusters or the bulk. Experimental results indicate relatively small magnetic moment per atom [$(0.3–1.4)\mu_B$/atom] with local minima at Mn_{13} and Mn_{19} and maxima at Mn_{15} and Mn_{23}–Mn_{25} [14]. Theoretical calculations of the structure and magnetic properties of Mn clusters containing 13, 15, 19, and 23 atoms show that Mn clusters possess complex spin configurations in which blocks of ferromagnetically coupled spins are antiferromagnetically coupled to each other [25].

Compared to the amount of work done for transition-metal clusters, little effort has been devoted to systematic investigation of magnetism in rare-earth-metal clusters, in spite of the fact that rare-earth metals possess remarkable magnetic properties. The heavy rare-earth elements, such as, Gd, Tb, Dy, Ho are ferromagnets in the bulk state. The magnetic moments of the rare-earth metals are dominated by the spin contribution from the highly localized $4f$ electrons, and therefore these metals are good examples of local-moment ferromagnets. The $4f$ electron shell can accommodate 14 electrons, and according to the empirical Hund's rule a half-filled shell has seven electrons with parallel spins. Thus, the $4f$ electrons contribute $7\mu_B$ to the total magnetic moment of Gd ($\sim 7.6\mu_B$/atom), and similarly make a large contribution to the total moments for the other magnetic rare-earth metals.

*On leave from Institute of Physics, St Petersburg State University, Ulianovskaya str. 1, 198504 St Petersburg, Petrodvorez, Russia; Email address: lyalin@fias.uni-frankfurt.de
†On leave from A. F. Ioffe Physical-Technical Institute, 194021 St. Petersburg, Russia.

The valence electrons contribute a small fraction of the overall magnetic moment per atom—in the case of bulk Gd, the $5d6s$ valence electrons contribute $0.6\mu_B$ of the total moment.

It has been demonstrated experimentally that the Gd_2 molecule is the diatomic molecule with the highest spin, which has in its ground state a magnetic moment $8.8\mu_B$/atom (compare with $6.5\mu_B$ for the free Gd atom, and $7.6\mu_B$/atom in the bulk metal) [26]. The recent Stern-Gerlach deflection experiments in Gd [27] and Dy [28,29] clusters showed enhancement of magnetism in small rare-earth-metal clusters. These investigations revealed that rare-earth clusters manifest interdependence between size, geometry and magnetism [30].

There are very limited number of theoretical works on rare-earth-metal clusters. In Ref. [30] the magnetic behavior of small rare-earth clusters with different geometries has been investigated within the quantum Heisenberg model. It has been shown that magnetic properties of heavy rare-earth clusters are highly dependent on the symmetry and geometry of the cluster. The *ab initio* density-functional theory (DFT) and Heisenberg model calculations have been performed for Gd_{13} cluster [31,32]. Calculations demonstrated that the ground state of the Gd_{13} cluster has C_{3v} symmetry and the local magnetic moments adopt a canted configuration [31,32]. This fact explains the reduction of the magnetic moment in small clusters.

It is important to note that even in a local-moment system such as rare-earth metals the behavior of the valence electrons is crucial because these electrons mediate the exchange interaction between neighboring magnetic moments localized on the parent atoms [22,33]. Lanthanum is the first element in the group of the rare-eath metals and its electronic configuration is $[Xe]4f^05d^16s^2$. Thus, La can be treated as a prototype of all rare-earth elements, sharing their properties that are not dependent upon $4f$ electrons. As the magnetic structures of the rare-earth metals are dependent on the occupancy of the $4f$ electron shell, they are absent from bulk La. Therefore, the emergence of magnetism in small La clusters remains an open question. Systematic theoretical investigations of magnetic properties of La clusters are lacking. In Ref. [34] energetics and structural stability of La clusters with number of atoms $N=3-13$ have been investigated by performing molecular dynamics simulations with an empirical pair potential. The potential energy function was fitted to the dimer potential energy profile of La_2, which was calculated by the DFT method [34]. The Möbius inversion pair potential in combination with genetic algorithm has been used in Ref. [35] in order to predict the lowest energy structures of the La_3-La_{20} clusters.

The first principles DFT calculations have been performed to study the electronic structure and spectroscopic constants of the La_2 dimer [36], as well as the structural and electronic properties of the icosahedral La_{13}, La_{13}^+, and La_{13}^- clusters [37]. The stable structures and electronic properties of small La_2-La_{14} clusters have been explored in Ref. [38].

Recently the magnetic properties of Sc, Y, and La clusters containing 5–20 atoms have been investigated in a Stern-Gerlach molecular-beam deflection experiment [39]. The results of experiment confirm that all Sc clusters and most Y and La clusters in the size range $N=5-20$ are elemental molecular magnets with particular strong enhancement of magnetism in $Sc_{13}[(6.0\pm0.2)\mu_B]$, $Y_8[(5.5\pm0.1)\mu_B]$, $Y_{13}[(8.8\pm0.1)\mu_B]$, and $La_6[(4.8\pm0.2)\mu_B]$ clusters [39].

In this paper we report the results of a systematic theoretical investigation of optimized ionic structure, electronic and magnetic properties of La clusters within the size range $N \leqslant 14$. We focus our study on emergence of magnetic properties in La clusters and found a giant enhancement of magnetism in La_4, La_6, and La_{13} clusters. We also found that the ground states of La_2, La_3, La_5, La_7, La_9-La_{11}, and La_{14} clusters possess nonzero magnetic moment, that ranged $\sim(0.1-1.0)\mu_B$ per atom, clearly indicating that small La clusters display magnetic behavior, even though bulk La has no magnetic ordering. We show that magnetism in La clusters is governed by unpaired valence electrons, in contrast to the local-moment magnetism in clusters of heavy rare-earth-metal elements. As already mentioned, the valence electrons are those that responsible for the local-moment spin coupling in rare-earth metals. Therefore, an understanding of the origin of magnetism in La clusters is important in order to gain a better insight of the magnetism of the rare-earth metal clusters. In addition to the ground state isomers of La clusters we found an ensemble of energetically low-lying spin isomers. We predict an increase of the average magnetic moments for ensembles of La_2, La_3, La_5, La_8, La_9, La_{11}, La_{12}, and La_{14} clusters with temperature due to the thermal population of the spin isomers. For ensembles of La_4, La_7, and La_{13} clusters the average magnetic moment decreases with temperature. Such an anomalous behavior of the magnetic moment with temperature can be detected in Stern-Gerlach deflection experiments.

II. THEORETICAL METHODS

Our calculations are based on *ab initio* theoretical methods invoking the density-functional theory. The standard LANL2DZ basis set of primitive Gaussians have been used to expand the cluster orbitals formed by the $5s^25p^65d^16s^2$ outer electrons of La (11 electrons per atom). The remaining 46 core electrons $1s^22s^22p^63s^23p^63d^{10}4s^24p^64d^{10}$ of the La atom are represented by the Wadt-Hay effective core potential (see, e.g., Refs. [40,41] and references therein). The computations are performed within the DFT method based on the gradient-corrected exchange-correlation functional of Perdew, Burke, and Ernzerhof (PBEPBE) [42,43]. Such an approach has proved to be a reliable tool for the *ab initio* level studying of the structure and properties of clusters of the alkali, the alkaline earth, and the transition metals. To check applicability of this method to lanthanum we performed a careful comparison of the results obtained with those of earlier *ab initio* and experimental studies.

The cluster geometries have been determined by finding local minima on the multidimensional potential energy surface. We have applied an efficient scheme of global optimization, called the cluster fusion algorithm [44,45]. The scheme has been designed within the context of determination of the most stable cluster geometries and it is applicable for various types of clusters [46]. Calculations have been carried out with the use of the GAUSSIAN 03 software package

[47]. With increasing cluster size, such calculations become computer time demanding. In this work, we limit the calculations by the cluster size $N=14$. The key point of the calculations is fixing the starting geometry of the cluster, which could converge during the calculation to a local or to the global energy minimum structure. In our calculations, we have created the starting geometries empirically, often assuming certain cluster symmetries. Note that during the optimization process, the geometry of the cluster as well as its initial symmetry sometimes change dramatically. All the characteristics of the clusters, which we have calculated and present in the following sections, are obtained for the clusters with optimized geometries. We have used similar approach to find the optimized geometries of the Na, Mg and Sr clusters [48–51].

III. NUMERICAL RESULTS AND DISCUSSION

A. Geometry structure of La_N clusters

We start our study with the lanthanum dimer, La_2. The investigation of the rare-earth-metal dimers is still a challenge for both experimentalists and theoreticians [56]. Although, several experimental [52–54] and theoretical [36,55–57] works on La_2 have been done, their results are not consistent with each other.

Our calculations show that the ground state of the La_2 dimer to be a triplet ($\mu=1\mu_B$), with dissociation energy $D_e=2.44$ eV, the bond length $d=3.00$ Å and the harmonic vibrational frequency $\omega_e=163$ cm^{-1}. The calculated dissociation energy is in excellent agreement with the experimental results of Refs. [52,53], where the value of 2.52 ± 0.22 eV was reported. The calculated value of the bond length, d, slightly overestimates the bond distance of 2.80 Å determined experimentally [52]. The calculated vibrational frequency, ω_e, underestimates significantly the measured ground state vibrational constant of 230 cm^{-1} [52]. We have also found several energetically close-lying spin isomers of La_2. The first spin isomer is found to be a pentet ($\mu=2\mu_B$), with the bond length of 3.10 Å; its dissociation energy of 2.42 eV only 0.02 eV lower than the ground state. The second isomer state is a singlet, with $d=2.94$ Å and $D_e=2.40$ eV.

The existence of a large number of energetically close-lying states makes the ground state determination to be a very difficult task. This fact can explain a large dispersion in theoretical results obtained by different methods. Thus, the first theoretical calculations of spectroscopic constants for La_2 were performed within configuration interaction method with inclusion single and double excitations and size-consistency error corrections (CISD+SCC)[57]. The calculations performed in Ref. [57] predicted a pentet ground state for La_2 and spectroscopic constants $d=3.25$ Å, $\omega_e=130$ cm^{-1}, $D_e=1.17$ eV in a strong disagreement with the current experimental data. In Ref. [34] spectroscopic constants of $d=3.28$ Å, $\omega_e=228$ cm^{-1}, $D_e=3.47$ eV were obtained for La_2 within an all-electron relativistic density-functional (RDFT) method. The bond distance and dissociation energy calculated within RDFT method for La_2 considerably overestimate those measured in the experiment.

The recent theoretical calculations for La_2 were performed with the use of the coupled cluster method with single, double and perturbative triple excitations [CCSD(T)] [56] and the complete active space self-consistent-field method (CASSCF) [55]. This calculation predicted the singlet to be a ground state of La_2 dimer. The theoretical values of $d=2.64$ Å $\omega_e=218$ cm^{-1}, $D_e=2.37$ eV, and $d=2.70$ Å, $\omega_e=186$ cm^{-1}, $D_e=2.31$ eV were obtained within CCSD(T) and CASSCF methods, respectively. The calculated values of dissociation energy and bond distance are in good agreement with experimental data, however, the vibrational frequency is underestimated. In Ref. [36] various DFT methods have been used for calculation of the spectroscopic constants for La_2. The calculated values of dissociation energy vary considerably among different DFT methods from 1.09 eV (BP86-LANL2DZ) to 3.66 eV (BHLYP-LANL2DZ) (see Table I in Ref. [36] for details). Overall results reported in Ref. [36] are in a poor agreement with experiment. In Ref. [38] dissociation energy of 3.08 eV and bond length of 2.77 Å were obtained for La_2 within the BLYP-DNP method.

In Table I we summarize results of our calculations of the spectroscopic constants for La_2 performed within the PBEPBE-LANL2DZ method, as well as the results reported in previous theoretical [34,36,38,55–57] and experimental [52,53] works. As it seen from Table I the PBEPBE-LANL2DZ estimation for La_2 dissociation energy is in excellent agreement with experimental data. The La_2 bond length calculated with the use of the PBEPBE-LANL2DZ method only slightly overestimates the experimental value of 2.80 Å [52]. This comparison allows us to conclude that the PBEPBE-LANL2DZ method is a reliable tool for the ab initio level studying the structure and properties of La clusters.

The results of the cluster geometry optimization for La clusters consisting of up to 14 atoms are shown in Fig. 1. La clusters possess various geometry and spin isomer forms whose numbers grow dramatically with increasing cluster size. In Fig. 1, we present only the lowest energy configurations optimized by the PBEPBE-LANL2DZ method. The interatomic distances are given in angstroms for La_2–La_7 clusters. The label above each cluster image indicates the point symmetry group of the cluster.

Figure 1 shows that small La clusters form compact structures, maximizing the coordination number. The lowest energy state for La_3 is a isosceles triangle, and for La_4 is a regular tetrahedron. La clusters are tri-dimensional already at $N>3$. As we discuss below, the La_4 cluster is relatively more stable and compact, as compared to the neighboring clusters. The La_5 cluster has a structure of slightly elongated triangular bipyramid, while La_6 has a structure of slightly flattened octahedron, La_7 is a pentagonal bipyramid. These geometrical structures are in a good agreement with the results of Ref. [38], except the case of La_4. We have found that regular tetrahedron structure T_d for La_4 has a lower energy than that of distorted tetrahedron structure C_s reported in Ref. [38]. This discrepancy can be explained by the fact that T_d structure found in this work, and C_s structure found in Ref. [38] are different spin isomers. We have found that the spin-nonet ($\mu=8\mu_B$) ground state becomes energetically more favorable for La_4 in comparison to the spin-triplet state considered in Ref. [38].

TABLE I. Magnetic moment, μ (units of μ_B), bond lengths, d (Å), vibrational frequencies, ω_e (cm^{-1}), and dissociation energies, D_e (eV), of the La_2 molecule.

Method	μ (units of μ_B)	d (Å)	ω_e (cm^{-1})	D_e (eV)
PBEPBE-LANL2DZ, this work	1	3.00	163	2.44
PBEPBE-LANL2DZ, this work	2	3.10	140	2.42
PBEPBE-LANL2DZ, this work	0	2.94	141	2.40
BP86-LANL2DZ [36]	0	2.93	139	1.09
B3LYP-LANL2DZ [36]	0	2.91	150	1.70
B3PW91-LANL2DZ [36]	0	2.89	131	1.83
PBE1PBE-LANL2DZ [36]	0	2.87	136	1.87
BHLYP-LANL2DZ [36]	0	2.87	161	3.66
RDFT [34]		3.28	228	3.47
CISD+SCC [57]	2	3.25	130	1.17
CASSCF [55]	0	2.70	186	2.31
CCSD(T) [56]	0	2.64	218	2.37
BLYP-DNP [38]	0	2.77		3.08
Experiment [52]		2.80	230	2.5±0.2
Experiment [53]				2.52±0.22

In the size region $N \geqslant 8$ the structures of clusters optimized with the use of the PBEPBE-LANL2DZ method are different from those derived on the basis of the BLYP-DNP approximation [38]. Thus, the lowest energy state for La_8 is a capped pentagonal bipyramid, C_s. The La_9 cluster has a low symmetry structure C_1 that is formed by fusion of deformed triangular bipyramid with strongly distorted rhombus, La_{10} has a C_{3v} structure, and La_{11} is a distorted D_{4d} structure. The La_{12} cluster is formed by fusion of a pentagonal bipyramid with a tetragonal pyramid, La_{13} is a regular icosahedron, and La_{14} has a C_s structure, which is close to slightly deformed C_{2v}. The structural stability of La_{13} has been already studied

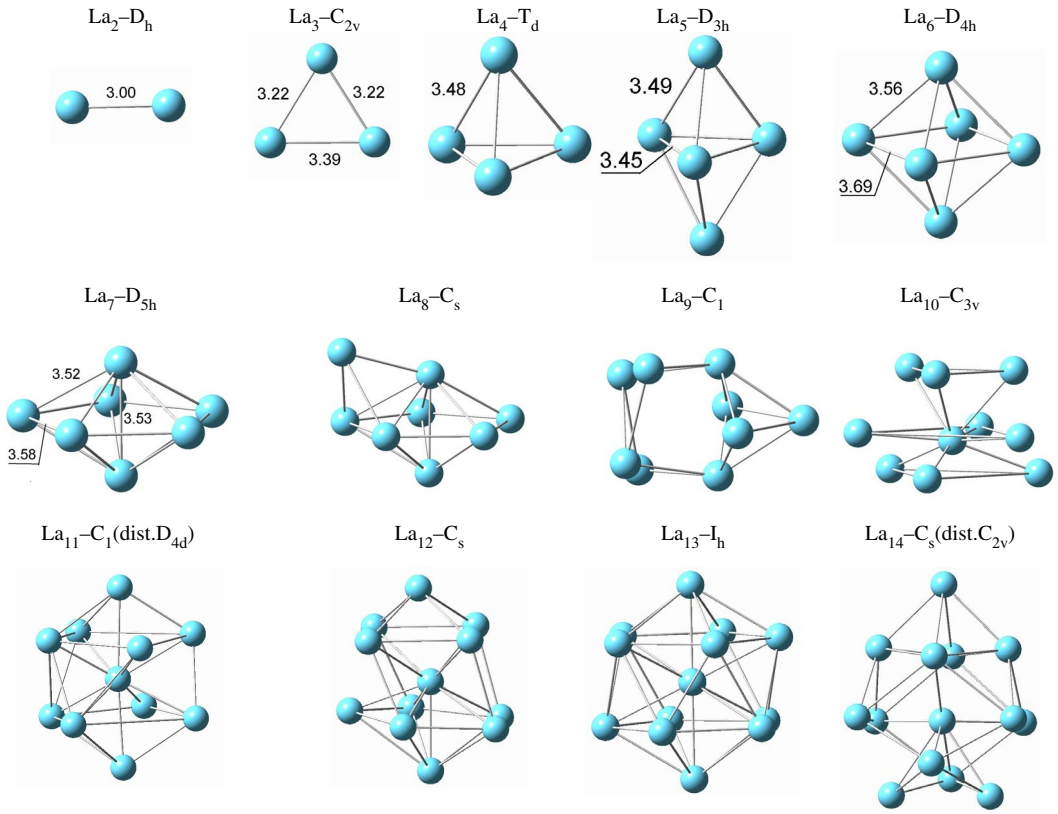

FIG. 1. (Color online) Optimized geometries of lanthanum clusters La_2–La_{14} calculated in the PBEPBE-LANL2DZ approximation. Interatomic distances are given in angstroms. Label above each cluster image indicates the point symmetry group of the cluster.

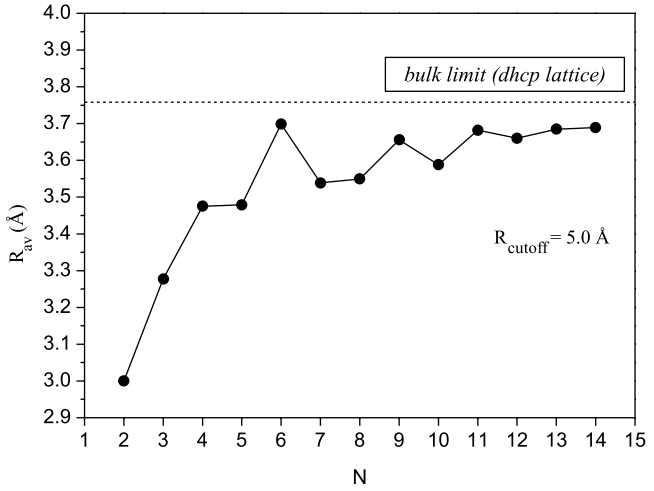

FIG. 2. Average bonding distance as a function of cluster size for La_2–La_{14} clusters. Horizontal dashed line indicates the bulk limit for the dhcp lattice of La [58].

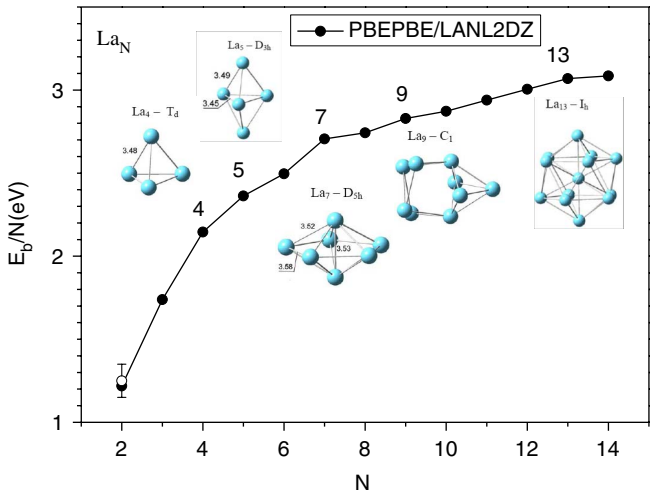

FIG. 3. (Color online) Binding energy per atom for the most stable La clusters as a function of cluster size. Open circle presents the binding energy per atom for La_2 dimer obtained from the experimental data by Verhaegen [52].

in Ref. [37]. It was found that the La_{13} cluster has its ground state of D_{2h} symmetry, while I_h and D_{3d} structures appear to be energetically close-lying isomers [37]. Our calculations show that the I_h structure (with the total spin $S=13/2$) is energetically more favorable in comparison with D_{2h} and D_{3d} structures. This disagreement is connected with difference in total spins of the ground states considered in Ref. [37] and in our work.

Figure 1 demonstrates a strong competition between icosahedral and octahedral growth motifs in the evolution of geometry structure of small La clusters with their size. The isocahedral packing is a typical growth motif for clusters of elements having van der Waals type of bonding, such as, for example, clusters of rare gases (see, e.g., Refs. [1,44]). A similar growth mode is also typical for clusters of alkaline earth metals, because the electronic shells in the divalent atoms are filled (the electronic configuration of the valence electrons is ns^2) and bonding between atoms is expected to have some features of the van der Waals type (see, e.g., Refs. [49–51] and references therein). The appearance of the octahedral elements in cluster structures is typical for the d transition metal clusters. The d orbitals have a square symmetry, and they can be responsible for formation of elements of a cubic lattice. Since lanthanum atom contains s and d valence electrons one can expect a competition between compact structures maximizing the number of bonds and directional bonding compatible with the orientation and filling of the d orbitals [1].

Figure 2 shows how the average bonding distance, R_{av}, evolves with increasing size of La clusters. The dependence of the average bonding distance on cluster size has nonmonotonic oscillatory behavior atop its fast systematic growth towards the bulk limit. In Fig. 2 the bulk limit for the double hexagonal closest-packing (dhcp) lattice of lanthanum is indicated by horizontal line. It is clearly seen in Fig. 2 that for $N \geqslant 11$ the average bonding distance for La clusters closely approaches the bulk limit. The appearance of the maxima in the size dependence of the average bonding distance shows that La_6, La_9, and La_{11} clusters are less compact than their neighbors. Exactly these structures possess elements of the cubic (or rhombic in the case of La_9) lattice as it is seen from Fig. 1. Therefore the oscillatory behavior of the average bonding distance can be interpreted by the competition between icosahedral and octahedral growth modes.

It is worth mentioning that the evolution of the average bonding distance with cluster size differs for La clusters from that for clusters of alkali and alkaline earth metals. Thus, for neutral alkali metal clusters, one can see odd-even oscillations of R_{av} atop its systematic growth and approaching the bulk limit [48]. These features have the quantum origin and arise due to the spin coupling of the delocalized valence electrons. For alkaline earth metal clusters, the average bonding distance depends on their size nonmonotonically. Such an irregular behavior is induced by both the closure of electronic shells of the delocalized electrons and the structural rearrangements [49].

B. Binding energy per atom for La_N clusters

The binding energy per atom for La clusters is defined as follows:

$$E_b/N = E_1 - E_N/N, \tag{1}$$

where E_N is the energy of a neutral N-particle atomic cluster, and E_1 is the energy of a single La atom.

Figure 3 shows the dependence of the binding energy per atom for the most stable lanthanum clusters as a function of cluster size.

For small La clusters the binding energy per atom increases steadily with the cluster size. The local maxima of E_b/N at $N=7$ and 13 correspond to the most stable configurations of the magic La clusters. The analysis of the second differences of the binding energy, $\Delta^2 E_N = E_{N+1} - 2E_N + E_{N-1}$, confirms this conclusion and makes a hint about relative stability of the La_4, La_5, and La_9 clusters, in addition to the magic clusters La_7, and La_{13} (see Fig. 4). The principal

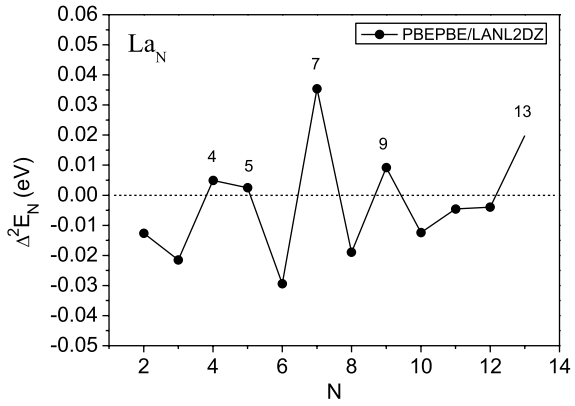

FIG. 4. Second differences of total energy for lanthanum clusters.

magic numbers 7 and 13 can be explained by atomic shells closings effects. Indeed, the enhanced stability of La_7 and La_{13} clusters arises when their ionic structure is highly symmetric and corresponds to the icosahedral type of packing. This icosahedral growth sequence for metal clusters has also been seen for clusters of alkaline earth metals such as Sr [50] and Ba [59], which exhibit nonmetal to metal transitions with increasing size. It is important to note that for alkaline earth metal clusters there is a strong competition between atomic and electronic shells closure [49,50]. However, for La clusters there is no direct influence of the electronic shell effects on cluster stability.

It is a typical feature of atomic clusters that they possess various isomer forms whose numbers grow dramatically with increasing cluster size. The important feature of La clusters consists in the fact that, in addition to structural isomers, they possess a great variety of energetically low-lying spin isomers. Figure 5 demonstrates the binding energies per atom calculated for a variety of low-lying geometry and spin isomers of La clusters. The typical difference in binding energy between the ground state and the first low-lying isomers is about 0.02–0.05 eV, as it is seen from Fig. 5. This result suggests that an ensemble of energetically low-lying isomers will be thermally available already at relatively low temperatures.

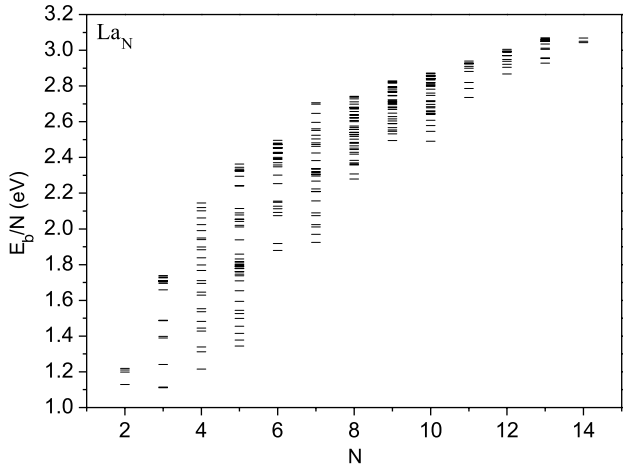

FIG. 5. Binding energy per atom for a variety of geometry and spin isomers of La clusters as a function of cluster size.

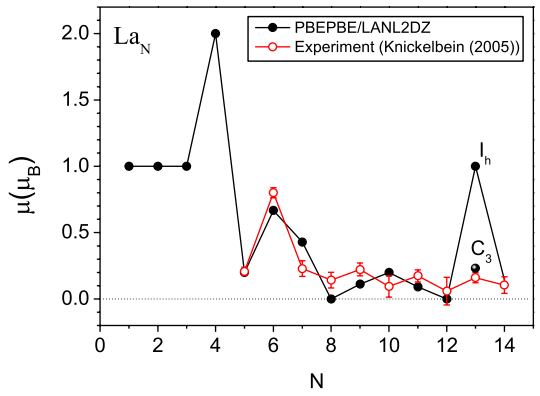

FIG. 6. (Color online) Magnetic moments per atom of La clusters as a function of cluster size. Filled circles represent the magnetic moments per atom calculated within the PBEPBE-LANL2DZ method. For La_{13}, the ground state structure I_h and the first low-lying isomer C_3 are presented. Open circles present the results of experiment by Knickelbein [39].

C. Magnetism of La_N clusters

The multitude of spin multiplicities, $2S+1$, for La clusters results in considerable variations of the magnetic moment per atom $\mu=2S\mu_B/N$. Figure 6 shows the dependence of the magnetic moment per atom for La clusters as a function of cluster size. Filled circles represent magnetic moments per atom calculated for the lowest energy isomers of La clusters. The calculations have been performed within the PBEPBE-LANL2DZ method. Open circles in Fig. 6 present the results of experiment by Knickelbein [39]. The magnetic moments reported in Ref. [39] were obtained for clusters generated at 58 ± 2 K.

Figure 6 shows that the dependence of the magnetic moment per atom, μ, on cluster size has complex and nonmonotonic behavior. For La_2 and La_3 clusters $\mu=1\mu_B$, that corresponds to ferromagnetic coupling of d electrons. Transition to three-dimensional (3D) structure for $N=4$ is accompanied by a giant enhancement of magnetism in La_4 ($\mu=2\mu_B$). The existence of an energetically favorable high-spin T_d structure for La_4 originates from the sd hybridization developing upon bonding. The results of our calculations demonstrate that an anomalous enhancement of magnetism also occurs in the highly symmetric La_6 (D_{4h}) and La_{13} (I_h) clusters. It is known that anomalous magnetism in low-dimensional transition metals can be attributed to the enhancement of densities of d states at the Fermi level resulting from spatial confinement [60]. For La clusters the effects of spatial confinement on magnetic properties can be explained by the Stoner model of itinerant ferromagnetism (see, e.g., Ref. [6] and references therein).

According to this model the total energy of the gas of itinerant electrons, E_{tot}, can be presented as a sum of Coulomb interaction energy, E_{Coul}, and kinetic energy, E_{kin},

$$E_{\text{tot}} = E_{\text{Coul}} + E_{\text{kin}}. \tag{2}$$

For a given number of electrons per atom $N_{\text{el}}=n_\uparrow+n_\downarrow$ and spin polarization, $n_\uparrow-n_\downarrow$, the Coulomb interaction energy per atom is given by

$$E_{\mathrm{Coul}} = \frac{1}{2}U(n_\uparrow + n_\downarrow)^2 - \frac{1}{2}J(n_\uparrow^2 + n_\downarrow^2)$$
$$= \frac{1}{2}\left(U - \frac{J}{2}\right)(n_\uparrow + n_\downarrow)^2 - \frac{J}{4}(n_\uparrow - n_\downarrow)^2. \quad (3)$$

Here U and J represent the average Coulomb repulsion between electrons having antiparallel spins and the exchange integral, respectively. The effective Coulomb repulsion between electrons with the same spin is reduced by the exchange integral. As it is seen from Eq. (3) the exchange interaction favors the ferromagnetic type of coupling. That corresponds to the first Hund's rule stating that the ground-state configuration of open-shell system has the largest possible total spin S (see, e.g., Ref. [6]). On the other hand, the kinetic energy, E_{kin}, associated to itinerant electrons in a cluster, favors equal filling of spin-up and spin-down states. In order to estimate E_{kin} for the given $n_\uparrow$ and $n_\downarrow$ one can introduce the spin polarization of the electron gas, by filling the lowest-energy k states having $\varepsilon_k < \varepsilon_F - \Delta$ for spin down, and $\varepsilon_k < \varepsilon_F + \Delta$ for spin up. Here ε_F is the Fermi level. Assuming that the density of states $N(\varepsilon)$ per spin depends weakly on ε for $|\varepsilon - \varepsilon_F| \leqslant \Delta$, one can obtain $n_\uparrow - n_\downarrow = 2\Delta N(\varepsilon_F)$ and

$$E_{\mathrm{kin}} = E_{\mathrm{kin}}^0 + N(\varepsilon_F)\Delta^2 = E_{\mathrm{kin}}^0 + \frac{(n_\uparrow - n_\downarrow)^2}{4N(\varepsilon_F)}, \quad (4)$$

where E_{kin}^0 is the kinetic energy of the spin unpolarized gas of electrons, with $n_\uparrow - n_\downarrow = 0$. According to Eq. (4) the increase of the kinetic energy E_{kin} due to the spin polarization becomes smaller with the growth of the density of states at the Fermi level, $N(\varepsilon_F)$, or with narrowing of the bandwidth [6]. From Eqs. (3) and (4) it is easy to obtain Stoner's criterion for ferromagnetic instability and spontaneous magnetic ordering,

$$JN(\varepsilon_F) > 1. \quad (5)$$

Thus, the Stoner model allows prediction of the emergence of anomalous magnetic ordering in clusters of transition elements (see, e.g., Ref. [39] and references therein). The spatial confinement leads to d-band narrowing [60] which produces an enhancement in $N(\varepsilon_F)$. This enhancement can lead to ferromagnetic instability and formation of spontaneous magnetic ordering in clusters.

It is also important to note that narrowing of d states in clusters can result from symmetry effects. Indeed, d states degenerate with increase in cluster symmetry, promoting ferromagnetic instability. It is clearly seen from Fig. 6 that the giant enhancement of magnetism occurs in the highly symmetric La_4 (T_d), La_6 (D_{4h} or distorted O_h) and La_{13} (I_h) clusters. On the other hand, the structural changes are often accompanied by strong changes in magnetic behavior. Thus, the reduction in symmetry of La_{13} from the ground state icosahedral structure to the first low-lying isomer with C_3 symmetry results in the sharp decrease in magnetic moment per atom from $1.0\mu_B$ to $0.23\mu_B$, respectively. Note that the difference in total binding energies between I_h and C_3 structures of La_{13} is only 0.06 eV.

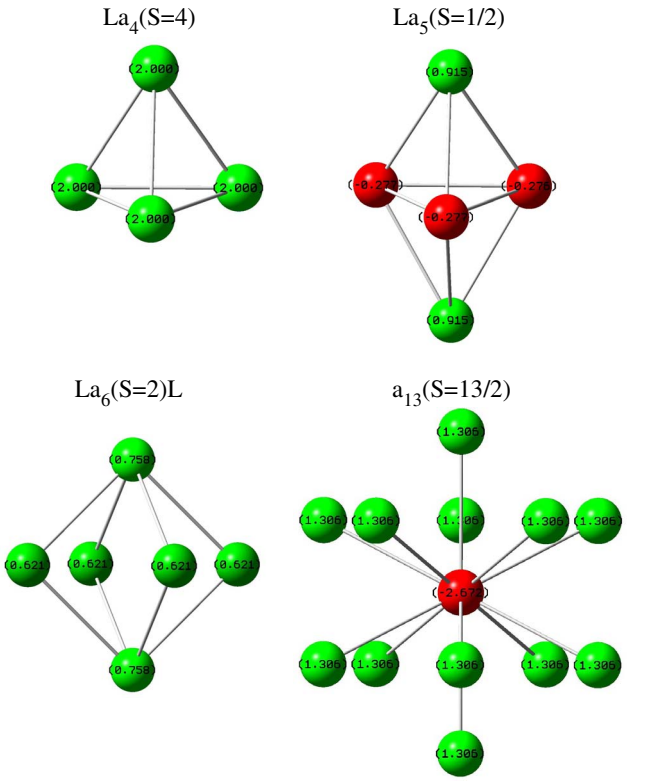

FIG. 7. (Color online) Mulliken atomic spin densities for La_4, La_5, La_6, and La_{13} clusters. The green and the red colors denote excess of spin-up and spin-down densities, respectively. The label above each cluster image indicates the total spin S of the cluster.

The Mulliken analysis of atomic spin densities demonstrate ferromagnetic ordering in La_4 and La_6 clusters as it is seen from Fig. 7. For La_{13} there is a ferromagnetic coupling within the surface atoms. However, the spin of the highly coordinated central atom is antiferromagnetically coupled with the spins of the surface atoms. This leads to a total magnetic moment per atom of $1.0\mu_B$ for the ground state of La_{13} cluster. The enhancement of the spin magnetization of La_{13} cluster is dominated by the surface contribution, even though the highest coordinated central atom has the highest moment, while the surface atoms have the lowest. It is interesting to note that magnetic ordering in La_{13} cluster is very different from that in icosahedral Mn_{13} cluster [25]. For Mn_{13} there is a ferromagnetic coupling within each of the five-membered rings as well as between each ring and its nearest neighbor cap. There is, however, an antiferromagnetic coupling between the rings. Additionally, the highly coordinated central atom is ferromagnetically coupled with one ring and antiferromagnetically coupled with the other [25].

Figure 6 demonstrates that the ground states of La_5, La_7, La_9–La_{11}, and La_{14} clusters possess nonzero magnetic moments, ranging from $\sim 0.1\mu_B$ to $0.5\mu_B$ per atom, clearly indicating that some La clusters display magnetic behavior, while clusters La_8 and La_{12} are not magnetic. The total magnetic moment of La clusters is comprised of sizable local atomic magnetic moments [$\sim(0.3-1.0)\mu_B$] that couple antiferromagnetically. For example, for La_5 there is a ferromagnetic coupling within three base atoms of triangular bipyra-

mid, and an antiferromagnetic coupling between the base and its capping atoms, as it is seen from Fig. 7.

Overall, the calculated magnetic moments of La clusters are in a good agreement with the experimental results of Ref. [39]. With an exception of $N=13$, the theoretical curve reproduces general features in the size dependence of the magnetic moment per atom obtained in experiment. The theory reproduces a giant enhancement of magnetism in La_6, discovered experimentally as well as it reproduces a sharp decrease in size dependence of μ for $N=7$ and 8. We found that the magnetic moments per atom are relatively small for La clusters within the size range $8 \leqslant N \leqslant 12$ in accord with the experiment. The calculated value of the magnetic moment for La_{12} is 0. This result is also in full agreement with the experiment that shows no measurable deflection or broadening of the beam profile for La_{12} [39]. Unfortunately, there are no experimental data for La_4, for which we predict a giant enhancement in magnetism, with the magnetic moment per atom reaching $2.0\mu_B$.

The main disagreement between the theory and the experiment arises for La_{13}. Figure 6 shows that theoretical value of the magnetic moment for the icosahedral La_{13} cluster considerably higher than observed in the experiment. Such a difference can arise due to the existence of energetically closely lying isomer structure of C_3 symmetry. The total binding energy, E_b, for the C_3 isomer of La_{13} cluster is only 0.06 eV smaller than that for the I_h ground state. The calculated magnetic moment per atom of $0.23\mu_B$ for C_3 isomer is in a good agreement with experiment, as it is seen from Fig. 6. We note that the size variation of the experimentally measured magnetic moment per atom of SC and Y clusters display pronounced maxima for $N=13$ [39]. By contrast, the experimental data for La_{13} displays no giant enhancement of magnetism. This difference was explained in Ref. [39] by possible different structural motifs in growth of SC, Y, and La clusters.

As we have discussed above, La clusters possess various structural and spin isomer forms. The small energy differences between spin isomers result in the dependence of the thermally averaged magnetic moment on temperature due to the thermal population of low-lying spin isomers.

Figure 8 shows the temperature dependence of the thermally averaged magnetic moment per atom, $\langle\mu\rangle$, which is defined as

$$\langle\mu\rangle = \frac{\sum_i \mu_i \exp(-E_i/kT)}{\sum_i \exp(-E_i/kT)}. \quad (6)$$

Here μ_i is the magnetic moment per atom for isomer i with the total energy E_i, k is the Boltzmann constant and T is the ensemble temperature.

The temperature dependence of $\langle\mu\rangle$ is expected to be rather weak for low temperatures $T<100-150$ K, and only the ground state isomer will contribute to $\langle\mu\rangle$ at the temperature of 58 K used in Ref. [39]. However, for $T>200-300$ K we found a strong dependence of the thermally averaged magnetic moment on temperature. Figure 8 demonstrates the increase of the average magnetic moments for ensembles of La_2, La_3, La_5, La_8, La_9, La_{11}, La_{12}, and La_{14} clusters with temperature which is due to the thermal population of the spin isomers. For the ensembles of La_4, La_7, and La_{13} clusters, the average magnetic moment decreases with temperature. For the ensembles of La_6 and La_{10} clusters the average magnetic moment practically does not depend on temperature up to $T=1000$ K. Such an anomalous behavior of the magnetic moment with temperature ($T>300$ K) can be detected in Stern-Gerlach deflection experiments. We believe we can explain the thermal behavior of La_2 dimer. The increase in temperature depopulates the triplet state and populate the pentet and the singlet states. Therefore, we predict that for La_2 a rise in temperature would lead first to increase of the thermally averaged magnetic moment per atom due to the increase in population of the pentet state. The subsequent decrease in $\langle\mu\rangle$ ($T>300$ K) would result from the higher population of the singlet state. Similar anomalous behavior of the magnetic moment has been predicted for small Pd clusters [61].

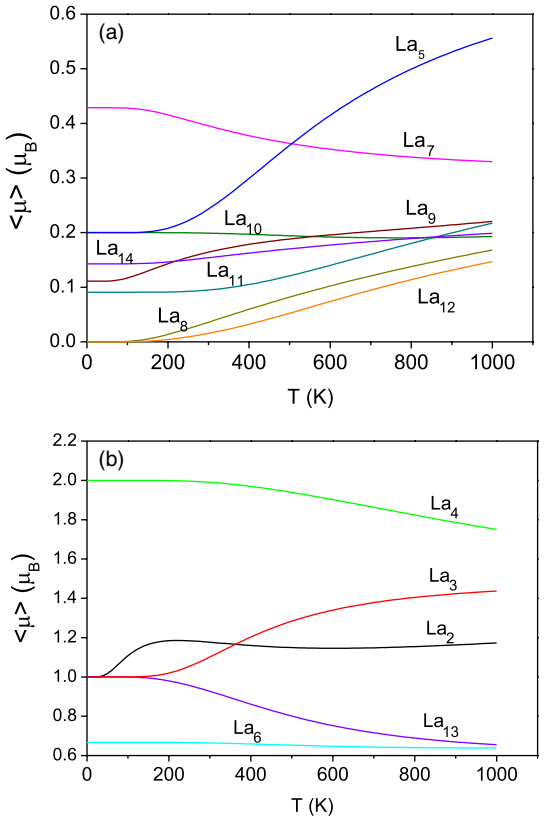

FIG. 8. (Color online) Thermally averaged magnetic moments per atom for La clusters.

IV. CONCLUSION

The optimized structure, electronic and magnetic properties of La clusters consisting of up to 14 atoms have been investigated using *ab initio* DFT PBEPBE-LANL2DZ method.

We found a giant enhancement of magnetism in La_4, La_6, and La_{13} clusters. We also found that the ground states of

La_2, La_3, La_5, La_7, La_9–La_{11}, La_{14} clusters possess nonzero magnetic moment, ranging from $\sim 0.1\mu_B$ to $1.0\mu_B$ per atom, clearly indicating that small La clusters display magnetic behavior, even though bulk La has no magnetic ordering. The results of our calculations of the magnetic moment per atom for La clusters are in a good agreement with those derived from experiment.

We show that increase in cluster symmetry can promote ferromagnetic instability in La clusters. On the other hand, the structural changes can be accompanied by strong changes in magnetic behavior.

A variety of structural and spin isomers were determined. We predict increase of the average magnetic moments for the ensembles of La_2, La_3, La_5, La_8, La_9, La_{11}, La_{12}, and La_{14} clusters with temperature for $T > 300$ K due to the thermal population of spin isomers. For the ensembles of La_4, La_7, and La_{13} clusters, the average magnetic moment decreases with temperature. Our study suggests temperature-dependent Stern-Gerlach deflection measurements.

Our results were obtained for free La clusters. Many interesting problems laying beyond the scope of the present work arise, however, when considering possible enhancement of magnetism in clusters deposited on a surface or embedded into a matrix. This problem can have important technological applications for the creation of new nanostructured materials with unique magnetic properties.

ACKNOWLEDGMENTS

This work is partially supported by the European Commission within the Network of Excellence project EXCELL, and by INTAS under the Grant No. 03-51-6170. The authors gratefully acknowledge support by the Frankfurt Center for Scientific Computing.

[1] J. A. Alonso, *Structure and Properties of Atomic Nanoclusters* (Imperial College Press, London 2005).
[2] *Atomic Clusters and Nanoparticles*, NATO Advanced Study Institute, les Houches Session LXXIII, les Houches, 2000, edited by C. Guet, P. Hobza, F. Spiegelman, and F. David (EDP Sciences and Springer Verlag, Berlin, 2001).
[3] *Latest Advances in Atomic Cluster Collisions: Fission, Fusion, Electron, Ion and Photon Impact*, edited by J.-P. Connerade and A. V. Solov'yov (Imperial College Press, London 2004).
[4] P.-G. Reinhard and E. Suraud, *Introduction to Cluster Dynamics* (Wiley-VCH, Weinheim, 2004).
[5] F. Baletto and R. Ferrando, Rev. Mod. Phys. **77**, 371 (2005).
[6] See G. M. Pastor in Ref. [2].
[7] N. Fujima and T. Yamaguchi, Phys. Rev. B **54**, 26 (1996).
[8] D. R. Salahab and R. P. Messmer, Surf. Sci. **106**, 415 (1981).
[9] K. Lee, J. Callaway, and S. Dhar, Phys. Rev. B **30**, 1724 (1985).
[10] S. N. Khanna and S. Linderoth, Phys. Rev. Lett. **67**, 742 (1991).
[11] T. Oda, A. Pasquarello, and R. Car, Phys. Rev. Lett. **80**, 3622 (1998).
[12] W. A. de Heer, P. Milani, and A. Chatelain, Phys. Rev. Lett. **65**, 488 (1990).
[13] J. P. Bucher, D. C. Douglass, and L. A. Bloomfield, Phys. Rev. Lett. **66**, 3052 (1991).
[14] M. B. Knickelbein, Phys. Rev. Lett. **86**, 5255 (2001).
[15] M. R. Pederson, F. Reuse, and S. N. Khanna, Phys. Rev. B **58**, 5632 (1998).
[16] N. Desmarais, F. A. Reuse, and S. N. Khanna, J. Chem. Phys. **112**, 5576 (2000).
[17] C. A. Bauman, R. J. Van Zee, S. Bhat, and W. Weltner, J. Chem. Phys. **78**, 190 (1983).
[18] R. J. Van Zee and W. Weltner, J. Chem. Phys. **89**, 4444 (1988).
[19] A. Terasaki, T. M. Briere, M. Kulawik, S. Minemoto, K. Tono, A. Matsushita, and T. Kondow, J. Chem. Phys. **118**, 2180 (2003).
[20] N. O. Jones, S. N. Khanna, T. Baruah, and M. R. Pederson, Phys. Rev. B **70**, 045416 (2004).
[21] S. K. Nayak and P. Jena, Chem. Phys. Lett. **289**, 473 (1998).
[22] C. Kittel, *Introduction to Solid State Physics*, 7th ed. (Wiley, New York, 1996).
[23] D. Hobbs and J. Hafner, J. Phys.: Condens. Matter **13**, L681 (2001).
[24] S. N. Khanna, B. K. Rao, P. Jena, and M. Knickelbein, Chem. Phys. Lett. **378**, 374 (2003).
[25] T. M. Briere, M. H. F. Sluiter, V. Kumar, and Y. Kawazoe, Phys. Rev. B **66**, 064412 (2002).
[26] R. J. Van Zee and W. Weltner, J. Chem. Phys. **100**, 4010 (1994).
[27] D. Gerion, A. Hirt and A. Châtelain, Phys. Rev. Lett. **83**, 532 (1999).
[28] S. Pokrant, Phys. Rev. A **62**, 051201(R) (2000).
[29] S. Pokrant and J. A. Becker, J. Magn. Magn. Mater. **226-230**, 1921 (2001).
[30] F. López-Urías, A. Díaz-Ortiz, and J. L. Morán-López, Phys. Rev. B **66**, 144406 (2002).
[31] D. P. Pappas, A. P. Popov, A. N. Anisimov, B. V. Reddy, and S. N. Khanna, Phys. Rev. Lett. **76**, 4332 (1996).
[32] V. Z. Cerovski, S. D. Mahanti, and S. N. Khanna, Eur. Phys. J. D **10**, 119 (2000).
[33] S. D. Barrett and S. S. Dhesi, *The Structure of Rare-Earth Metal Surfaces* (Imperial College Press, London 2001).
[34] S. Erkoc, T. Bastug, M. Hirata, and S. Tachimori, Chem. Phys. Lett. **314**, 203 (1999).
[35] Y.-H. Luo and Y. Wang, Phys. Rev. A **64**, 015201 (2001).
[36] Z.-J. Wu, J. S. Shi, S. Y. Zhang, and H. J. Zhang, Phys. Rev. A **69**, 064502 (2004).
[37] D.-B. Zhang and J. Shen, J. Chem. Phys. **120**, 5081 (2004).
[38] D.-B. Zhang and J. Shen, J. Chem. Phys. **120**, 5104 (2004).
[39] M. B. Knickelbein, Phys. Rev. B **71**, 184442 (2005).
[40] James B. Foresman and Æleen Frisch *Exploring Chemistry with Electronic Structure Methods* (Gaussian Inc., Pittsburgh, PA, 1996).
[41] P. J. Hay and W. R. Wadt, J. Chem. Phys. **82**, 299 (1985).
[42] J. P. Perdew, K. Burke, and M. Ernzerhof, Phys. Rev. Lett. **77**, 3865 (1996).

[43] J. P. Perdew, K. Burke, and M. Ernzerhof, Phys. Rev. Lett. **78**, 1396 (1997).
[44] A. Koshelev, A. Shutovich, I. A. Solov'yov, A. V. Solov'yov, and W. Greiner, Phys. Rev. Lett. **90**, 053401 (2003).
[45] I. A. Solov'yov, A. V. Solov'yov, and W. Greiner, Int. J. Mod. Phys. E **13**, 697 (2004).
[46] O. I. Obolensky, I. A. Solov'yov, A. V. Solov'yov, and W. Greiner, Comput. Let. **1**, 313 (2005).
[47] M. J. Frisch *et al.*, GAUSSIAN 03, Rev. C.02, Gaussian Inc., Wallingford, CT, 2004.
[48] I. A. Solov'yov, A. V. Solov'yov, and W. Greiner, Phys. Rev. A **65**, 053203 (2002).
[49] A. Lyalin, I. A. Solov'yov, A. V. Solov'yov, and W. Greiner, Phys. Rev. A **67**, 063203 (2003).
[50] A. Lyalin, A. V. Solov'yov, C. Bréchignac, and W. Greiner, J. Phys. B **38**, L129 (2005).
[51] See I. A. Solov'yov, A. Lyalin, A. V. Solov'yov, and W. Greiner, in Ref. [3].
[52] G. Verhaegen, S. Smoes, and J. Drowart, J. Chem. Phys. **40**, 239 (1964).
[53] J. A. Connor, in *Metal Clusters in Catalysis: Studies in Surface Science and Catalysis*, edited by B. A. Gates, L. Guczi, and L. H. Knoezinger (Elsevier, Amsterdam, 1986), Vol. 29.
[54] Y. Liu, Li Fang, X. Shen, X. Chen, J. R. Lombardi, and D. M. Lindsay, Chem. Phys. **262**, 25 (2000).
[55] X. Cao and M. Dolg, Theor. Chem. Acc. **108**, 143 (2002).
[56] X. Cao and M. Dolg, Mol. Phys. **101**, 1967 (2003).
[57] M. Dolg, H. Stroll, and H. Preuss, J. Mol. Struct.: THEOCHEM **277**, 239 (1992).
[58] B. J. Beaudry and K. A. Gschneidner, in *Handbook on the Physics and Chemistry of Rare Earths*, edited by K. A. Gschneidner and L. Eyring (North-Holland, Amsterdam, 1978), Vol. 1.
[59] Q. Wang, Q. Sun, J.-Z. Yu, B.-L. Gu, Y. Kawazoe, and Y. Hashi, Phys. Rev. A **62**, 063203 (2000).
[60] F. J. Himpsel, J. E. Ortega, G. J. Mankey, and R. F. Wills, Adv. Phys. **47**, 511 (1998).
[61] M. Moseler, H. Häkkinen, R. N. Barnett, and U. Landman, Phys. Rev. Lett. **86**, 2545 (2001).